7

Internal Design of the Dry Human Ulna by DXA

S. Aguado-Henche, A. Bosch-Martín,
P. Spottorno-Rubio and R. Rodríguez-Torres
University of Alcalá
Spain

1. Introduction

Dual energy X-ray absorptiometry (DXA) has been used to study dry bones such as spine, femur, jaw... to detect the first onsets of the ossification centers; In clinical practice, DXA is widely used for diagnosis and evaluation of osteoporosis, and a new generation of DXA scanners offers software for performing vertebral morphometry analysis (Blake & Fogelman, 1997). Also, many bone analyses have been performed on experimental animals using DXA (Tsujio et al., 2009).

Studies on the spatial distribution of bone mineral density (BMD) in the whole bone, reflecting its morphological pattern are scarce (Gómez-Pellico et al., 1993 & Fernández-Camacho et al., 1996). In addition, there are just few studies regarding the anthropometric characteristics of the human ulna (Weber et al., 2009).

In order to improve the treatment of the elbow's injury, knowledge related to the resistance of the bone is important to understand the origin of the fractures as well as to improve elbow fracture recovery (Heep, 2007). Most studies investigate the humeral component, while the ulna component is not being studied as much (Goto, 2009).

In order to develop an implant that carries out the mechanical characteristics of a native bone, we must study the trabecular architecture of the human ulna proximal extremity.

1.1 Brief anatomy of the human ulna

The ulna is a long bone, placed at the medial side of the forearm, parallel to the radius. It is divisible into a body and two extremities. Its upper extremity, of great thickness and strength, forms a large part of the elbow-joint; the bone diminishes in size from above downward, its lower extremity being very small, and excluded from the wrist-joint by the interposition of an articular disk (the ulna articulates with the humerus and radius).

The upper extremity presents two curved processes, the olecranon and the coronoid process; and two concave, articular cavities, the trochlear and radial notches. The olecranon is a large, thick, curved eminence, situated at the upper and back part of the ulna. The coronoid process is a triangular eminence projecting forward from the upper and front part of the ulna. Its base is continuous with the body of the bone, and of considerable strength.

Its antero-inferior surface is concave, and marked by a rough impression for the insertion of the brachialis muscle. The trochlear notch is a large depression, formed by the olecranon and the coronoid process, and serving for articulation with the trochlea of the humerus. The notch is concave from above downward, and divided into a medial and a lateral portion by a smooth ridge running from the summit of the olecranon to the tip of the coronoid process. The radial notch is a narrow, oblong, articular depression on the lateral side of the coronoid process; it receives the circumferential articular surface of the head of the radius. The lower extremity of the ulna is small, and presents two eminences; the lateral and larger is a rounded, articular eminence, termed the head of the ulna; the medial, narrower and more projecting is a non-articular eminence named the styloid process.

The ulna is ossified from three centers: one for the body, the inferior extremity, and the top of the olecranon. Ossification begins about the eighth week of fetal life. About the fourth year, a center appears in the middle of the ulnar head, and soon extends into the styloid process. About the tenth year, a center appears in the olecranon near its extremity. The upper epiphysis joins the body about the sixteenth year and the lower about the twentieth.

2. Objective

In this chapter, we set out to show, by means of densitometric analysis with dual energy X-ray absorptiometry (DXA) the internal design of the human ulna, to verify that the bone tissue distribution is not homogeneous and that this corresponds to the trabecular architecture of the bone.

3. Material and method

A random sample of 41 dry right ulnas from the skeletal collection of the Anatomy and Embriology Department of the University of Alcala was studied excluding those bones which presented any alterations or damage. A Norland XR-26 densitometer, software 2.5 (Norland Co., Fort Atkinson, WI, USA; Emsor SA, Madrid) was used for all studies. Each scan session was preceded by a calibration routine using a standard calibration block supplied by the manufacturer.

The bone is placed well centred on the examining board. It is important to check for stability so as not to vary its position during the study. Cotton gauze may be needed for an optimal stabilization. The bones are exposed directly, without any water or other materials that may resemble soft tissue.

For the densitometric analysis of the human ulna structure two projections were performed: lateral and antero-posterior.

For the study in two positions, the reference will be the ridge of the trochlear notch of the epiphyseal ulna (incisura trochlearis) which corresponds to the throat of the trochlea –humerus- (Gómez-Oliveros, 1962).

- Anteroposterior Position: The axis of the ridge of the trochlear notch is perpendicular to the axis of the examining board.
- Lateral Position: The axis of the ridge of the trochlear notch is parallel to the axis of the examining board.

To begin the scan, (figure 1) the starting point was placed 0, 5 cm directly above the upper extremity. A baseline point was marked under the lower extremity. A third point (goal line) was marked 1 cm from the more lateral part of the bone.

Fig. 1. Definition of the exploration area

This technique has high accuracy and precision, approaching 1%. The speed of scanning was 60 mms, with an interlinear space of 1 mm and point by point resolution of 1 mm horizontal x 1 mm vertical. The defined exploration was completed as outlined in an average time of 10-15 min. Scan acquisition and scan analyses were performed by one investigator (figure 2).

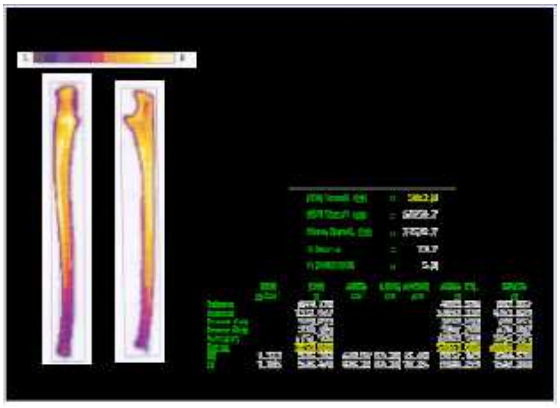

Fig. 2. Densitometric image of the ulna.

Dry ulna calculations were performed for the following magnitudes:

BMD: Bone mineral density, in grams / cm^2.

BMC: Bone mineral content, in grams. BMC is defined as the mass of mineral contained in an entire bone or as the mass of mineral per unit bone length. Bone mineral content is obviously a size-dependent parameter (Schoenau, 2004).

AREA: Measured area, in square centimetres (cm^2).
LENGTH: Total length of the bone, in centimetres (cm).
WIDTH: Total width of the bone, in centimetres (cm).

For the purpose of this survey, in both projections five equal regions of interest (ROI) were selected: proximal (ROI-1), proximal-intermediate (ROI-2), intermediate (ROI-3), distal-intermediate (ROI-4) and distal (ROI-5). The total region corresponded to the area of the full length and height of the bone (figure 3).

All statistical calculations were performed using Statgraphics Plus (version 5.1) and SPSS (Statistical Package for Social Sciences), version 15.0. The means and standard deviation (SD) for bone mineral density (BMD) and bone mineral content (BMC) were calculated. The bone densities and the bone contents of the various regions of the ulna in the 2 projections were compared by Student's *t* test for paired samples.

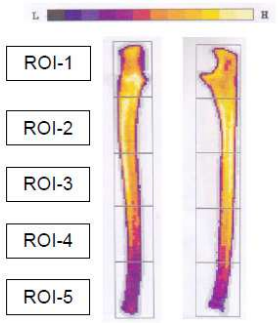

Fig. 3. Regions of interest.

4. Results

DXA indicates that the higher BMD is in the proximal-intermediate region (R2), which is the part of the ulna that bears the higher force of traction. The higher BMC is found in the proximal region (R1) which corresponds to the coronoid process. Lower BMD and BMC are found in the distal region (R5). The total BMD shows significant statistical differences ($p \leq 0.001$), which indicates the heterogeneous nature of the distribution of bone mass in the studied bone.

In tables 1 - 4 we present the statistic descriptions of the densitometry variables studied in both.

Projection A-P	Mínimum	Máximum	Mean	SD
Total BMD	0,40	0,97	0,69	0,14
Total BMC	13,10	46,40	28,75	8,63
Total Area	30,73	51,54	41,05	5,70
Total Lenght	20,40	27,90	24,51	1,66
Total Width	2,55	4,35	3,35	0,40

Table 1. Descriptive statistics of the total ulna in projection antero-posterior (n=41). SD: Standard deviation.

Projection LAT	Mínimum	Máximum	Mean	SD
Total BMD	0,38	0,94	0,67	0,14
Total BMC	13,15	46,74	28,72	8,50
Total Area	32,81	52,51	41,84	5,25
Total Lenght	20,40	28,05	24,50	1,66
Total Width	3,15	6,60	4,08	0,59

Table 2. Descriptive statistics of the total ulna in projection lateral (n=41). SD: Standard deviation.

	ROI 1		ROI 2		ROI 3		ROI 4		ROI 5	
	Media	SD	Media	SD	Media	SD	Media	SD	Media	SD
AP-Area	10,58	1,57	9,08	1,33	8,12	1,42	7,02	1,01	6,22	0,94
AP-Lenght	4,88	0,33	4,88	0,33	5,03	0,41	4,88	0,33	4,88	0,33
LAT-Area	11,68	1,52	8,94	1,24	8,09	1,07	6,98	0,82	6,24	1,00
LAT-Lenght	4,88	0,33	4,88	0,33	5,03	0,43	4,88	0,33	4,88	0,33

Table 3. Descriptive statistics of the regions of interest in projections antero-posterior (AP) and lateral (LAT). n=41. SD: Standard deviation.

ANTERO-POSTERIOR VIEW			LATERAL VIEW	
BMD	BMC		BMD	BMC
0,754	8,136	ROI-1	0,678	8,07
0,81	7,513	ROI-2	0,819	7,442
0,734	6,089	ROI-3	0,750	6,169
0,599	4,289	ROI-4	0,608	4,297
0,447	2,814	ROI-5	0,453	2,819
ULNA TOTAL BMD 0,69			ULNA TOTAL BMD 0,67	
ULNA TOTAL BMC 28,75			ULNA TOTAL BMC 28,72	

Table 4. BMD (in grams/cm^2) and BMC (in grams) of the regions of interest.

5. Discussion

Dual energy X-ray absorptiometry (DXA) allows us to gather quantitative information on bone mineral content (BMC) and bone mineral density (BMD) of the bone (Wahner et al., 1985). As previously reported (Hvid et al., 1985), there is a close relationship between bone mass and bone strength.

In literature, there are various studies on long bones, such as the femur, the tibia, the humerus and the radius (Wahner et al., 1985; Kawashima & Uhthoff, 1991; Gómez-Pellico et

al., 1993; D'Amelio et al., 2002) but we haven't found any references that study the distribution of the BMD in the ulna that describes it´s construction systematics .

According to Wolf's law (Viladot , 2001), the bone adapts its size, shape and structure to the mechanical requirements it receives. Furthermore, Pauwels (Pauwels, 1980; Miralles, 1998) suggests that the mass of the cortical bone is distributed along its axis proportionally to the amount of tensions it receives. In our analysis, we find a wider BMD in the intermediate-proximal region (ROI-2), which corresponds to the region of the bone exposed to the mechanical flexions and to the transmission of weight charges while the superior member is in the extended position. Three different soft tissue structures insert in or attach to the coronoid process, the articular capsule, the tendon of the brachialis muscle, and the anterior band of the ulnar collateral ligament (Fowler & Chung, 2006). Furthermore, the transmission of weight charges travels through the coronoid apophysis, situated in the proximal region, which present the wider BMC in both projections, however, DXA is unable to distinguish between cortical and trabecular bone (Griffith & Genant, 2008).

This and other similar studies will contribute to a better understanding of stress related fractures which are quite scarce in the ulna and cannot easily be found in literature (Chen, WC et al., 1991). Most fractures occur in the middle third of the diaphysis and surrounding areas as a result of mechanical stressing forces of the forearm in a specific position, especially in athletes (Rettig, 1983).

Some authors have agreed on the homogeneous nature of the different diaphysarial regions of the long bones that they study (femur, humerus and tibia) (Gómez Pellico et al., 1993; Fernández-Camacho et al., 1996). As far as the ulna is concerned, BMD displays a more heterogeneous distribution, since we find statistical differences in all studied regions and on the entire bone.

In studies of the dry femur with DXA, epiphysiary regions are those with less BMD which, added to the mechanical requirements of the physiology of the articulation, would explain how hip ostheoporotic fractures occur (Gómez-Pellico et al., 1993). Furthermore, most studies with DXA are based on BMD variations related to loss of bone mass of pathologic nature (McCarthy et al., 1991). This also happens with "in vivo" studies of the radius. Due to the high rate fractures of the distal radius in children, the use this bone to measure BMD, is increasing, essentially as thus to predict the risk of fracture (Kalkwarf et al., 2011). The study of the dry radius with DXA would define its construction systematics.

The results obtained with the DXA technique showed that BMD agrees with the arrangement of the trabecular system in the human ulna, previously described by some authors (Testut & Latarjet, 1949; Gómez-Oliveros, 1962).

In addition, fractures of the coronoid process are rarely seen as an isolated injury. They are encountered more frecuently in association with radial head fractures (Weber et al., 2009).

Due to frequent complications associated with reconstructive surgery for the elbow, implant loosening, periprosthetic fracture, implant failure… (Kim, 2011), that remains higher than arthroplasty of other joints (Sanchez-Sotelo, 2011), the findings that result from this study could contribute to the improvement of elbow prosthesis.

6. Conclusions

The human ulna presents a heterogeneous distribution of the BMD. This study confirms that the higher mechanical requirements in the ulna are in the proximal extremity. The differences found in the ulna BMD allows us a better understanding of the construction systematics and their functional activity. We conclude that bone densitometry, measured by the DXA technique, is useful for assessing trabecular architecture of the human skeleton. This study may provide some useful information on plate application for the treatment of the elbow injuries.

7. References

Blake, GM. & Fogelman I. (1997). Technical principles, *Seminars in Nuclear Medicine* 27(3):210-228.

D'Amelio, P., Panattoni, GL. & Isaia GC. (2002). Densitometric study of human developing dry bones: a review, *Journal of Clinical Densitometric* 5(1):73-78.

Chen, WC., Hsu, WY & Wu, JJ (1991). Stress fracture of the diaphysis of the ulna, *International Orthopaedics* 15: 197-198.

Fernández Camacho, FJ., Morante Martínez, P., Rodríguez Torres, R., Cortés García, A. & Gómez Pellico, L. (1996). Densitometric analysis of the human calcaneus, *Journal of Anatomy* 189:205-209.

Fowler, K. & Chung, C. (2006). Normal MR imaging anatomy of the elbow, *Radiologic Clinics of North America* 44(4):553-567.

Gómez Pellico, L., Morante Martínez, P., & Dankloff Mora, C. (1993). Definición densitométrica de la morfología estructural del huesos del esqueleto humano, *Jano* XLV:637-640.

Gómez-Oliveros, L. (1962). *Lecciones de Anatomía Humana. Osteología. Tercera parte. Miembros.* Madrid. Marban.

Goto, A., Murase, T., Hashimoto, J., Oka, K., Yoshikawa, H. & Sugamoto, K. (2009). Morphologic análisis of the medulary canal in rheumatoid elbows, *Journal of Shoulder and Elbow Surgery.*18(1):33-37.

Griffith, JF., Genant, HK. (2008). Bone mass and architecture determination: state of the art, *Best practice & Research Clinical Endocrinology & Metabolism.*22(5):737-764.

Hepp, P., Josten, C. (2007). Biology and Biomechanics in Osteosynthesis of Proximal Humerus Fractures, *European Journal of Trauma and Emergency Surgery* 33(4):337-344.

Hvid, I., Jensen, NC., Bünger, C., Solund, K., Djurhuus, JC. (1985). Bone mineral assay: its relation to the mechanical strength of cancellous bone, *Engineering in Medicine* 14:79-83.

Kalkwarf, HJ., Laor, T & Bean JA. (2011). Fracture risk in children with forearm injury is associated with volumetric bone density and cortical area (by peripheral QCT) and areal bone density (by DXA), *Osteoporosis International* 22:607-616.

Kawashima, T. & Uhthoff HK. (1991). Pattern of bone loss of the proximal femur: a radiologic, densitometric, and histomorphometric study, *Journal of Orthopaedic Research* 9(5):630-640.

Kim, JM., Mudgal, CS., Konopka, JF & Júpiter JB. (2011). Complications of total elbow arthroplasty, *Journal of American Academy of Orthopaedic Surgeons.* 19(6):328-339.

McCarthy, CK., Steinberg, GG., Agren, M., Leahey, D., Wyman, E., & Baran DT (1991). Quantifying bone loss from the proximal femur after total hip arthroplasty, *Journal of Bone and Joint Surgery* 73(5):774-778.

Miralles Marrero, R. (1998). *Biomecánica Clínica del Aparato Locomotor.* Barcelona: Masson.

Pauwels, F. (1980) *Biomechanics of the Locomotor Apparatus. Contribution on the functional of the Locomotor Apparatus.* Nueva York: Srpinger.

Rettig, AC. (1983). Stress fracture of the ulna in an adolescent tournament tennis player. *American Journal of Sports Medicine* 11:103-106.

Sanchez-Sotelo, J. (2011). Total elbow arthroplasty, *The Open Orthopaedics Journal* 16(5):115-123.

Schoenau, E., Land, C., Stabrey, A., Remer, T. & Kroke, A. (2004). The bone mass concept: problems in short stature, *European Journal of Endocrinology* 151:S87-S91.

Testut, L. & Latarjet, A. (1949). *Tratado de Anatomía Humana. Volume 1* Barcelona: Salvat.

Tsujio, M., Mizorogi, T., Kitamura, I., Maeda, Y., Nishijima, K., Kuwahara, S., Ohno, T., Niida, S., Nagoya, M., Saito, R. & Tanaka, S. (2009). Bone mineral analisis through dual energy X-ray absorptiometry in laboratory animals, *Journal of Veterinary Medical Science* 71(11):1493-1497.

Viladot Voegeli, A. (2001) *Lecciones Básicas de Biomecánica del Aparato Locomotor.* Barcelona: Springer.

Wahner, HW., Eastell, R. & Riggs, BL. (1985). Bone mineral density of the radius: Where do we stand?, *The Journal of Nuclear Medicine* 26(11):1339-1341.

Weber, MF., Barbosa, DM., Belentani, C., Ramos, PM., Trudell, D. & Resnick, D. (2009). Coronoid process of the ulna: paleopathologic and anatomic study with imaging correlation. Emphasis on the anteromedial "facet", *Skeletal Radiology* 38(1):61-67.

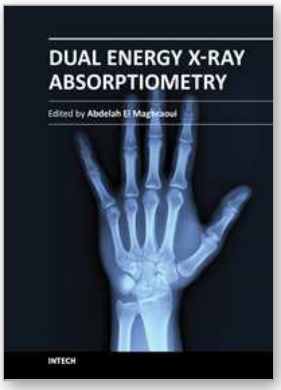

Dual Energy X-Ray Absorptiometry

Edited by Prof. Abdelah El Maghraoui

ISBN 978-953-307-877-9
Hard cover, 146 pages
Publisher InTech
Published online 25, January, 2012
Published in print edition January, 2012

The World Health Organization (WHO) has established dual-energy x-ray absorptiometry (DXA) as the best densitometric technique for assessing bone mineral density (BMD) in postmenopausal women and has based the definitions of osteopenia and osteoporosis on its results. DXA enables accurate diagnosis of osteoporosis, estimation of fracture risk and monitoring of patients undergoing treatment. Additional features of DXA include measurement of BMD at multiple skeletal sites, vertebral fracture assessment and body composition assessment, including fat mass and lean soft tissue mass of the whole body and the segments. This book contains reviews and original studies about DXA and its different uses in clinical practice (diagnosis of osteoporosis, monitoring of BMD measurement) and in medical research in several situations (e.g. assessment of morphological asymmetry in athletes, estimation of resting energy expenditure, assessment of vertebral strength and vertebral fracture risk, or study of dry bones such as the ulna).

InTech Europe
University Campus STeP Ri
Slavka Krautzeka 83/A
51000 Rijeka, Croatia
Phone: +385 (51) 770 447
Fax: +385 (51) 686 166
www.intechopen.com

InTech China
Unit 405, Office Block, Hotel Equatorial Shanghai
No.65, Yan An Road (West), Shanghai, 200040, China
中国上海市延安西路65号上海国际贵都大饭店办公楼405单元
Phone: +86-21-62489820
Fax: +86-21-62489821